Nanoscale c8nr10114k

We have presented the Graphical Abstract text and image for your article below. This brief summary of your work will appear in the contents pages of the issue in which your article appears.

1

Nano-hybrid electrospun non-woven materials made of wool keratin and hydrotalcites as potential bio-active wound dressings

Demetra Giuri, Marianna Barbalinardo, Giovanna Sotgiu, Roberto Zamboni, Morena Nocchetti, Anna Donnadio, Franco Corticelli, Francesco Valle, Chiara G. M. Gennari, Francesca Selmin, Tamara Posati* and Annalisa Aluigi*

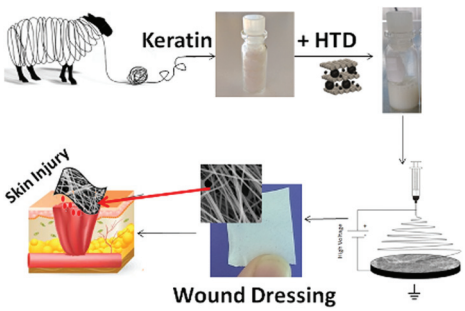

In this work, nano-hybrid electrospun non-woven materials made of wool keratin combined with diclofenac loaded hydrotalcites (HTD) were prepared and characterized as potential drug delivery systems and scaffolds for fibroblast cell growth.

Q4

Please check this proof carefully. Our staff will not read it in detail after you have returned it.

Please send your corrections either as a copy of the proof PDF with electronic notes attached or as a list of corrections. **Do not edit the text within the PDF or send a revised manuscript** as we will not be able to apply your corrections. Corrections at this stage should be minor and not involve extensive changes.

Proof corrections must be returned as a single set of corrections, approved by all co-authors. No further corrections can be made after you have submitted your proof corrections as we will publish your article online as soon as possible after they are received.

Please ensure that:

- The spelling and format of all author names and affiliations are checked carefully. You can check how we have identified the authors' first and last names in the researcher information table on the next page. **Names will be indexed and cited as shown on the proof, so these must be correct.**
- Any funding bodies have been acknowledged appropriately and included both in the paper and in the funder information table on the next page.
- All of the editor's queries are answered.
- Any necessary attachments, such as updated images or ESI files, are provided.

Translation errors can occur during conversion to typesetting systems so you need to read the whole proof. In particular please check tables, equations, numerical data, figures and graphics, and references carefully.

Please return your **final** corrections, where possible within **48 hours** of receipt, by e-mail to: nanoscale@rsc.org. If you require more time, please notify us by email.

Funding information

Providing accurate funding information will enable us to help you comply with your funders' reporting mandates. Clear acknowledgement of funder support is an important consideration in funding evaluation and can increase your chances of securing funding in the future.

We work closely with Crossref to make your research discoverable through the Funding Data search tool (http://search.crossref.org/funding). Funding Data provides a reliable way to track the impact of the work that funders support. Accurate funder information will also help us (i) identify articles that are mandated to be deposited in **PubMed Central (PMC)** and deposit these on your behalf, and (ii) identify articles funded as part of the **CHORUS** initiative and display the Accepted Manuscript on our web site after an embargo period of 12 months.

Further information can be found on our webpage (http://rsc.li/funding-info).

What we do with funding information

We have combined the information you gave us on submission with the information in your acknowledgements. This will help ensure the funding information is as complete as possible and matches funders listed in the Crossref Funder Registry.

If a funding organisation you included in your acknowledgements or on submission of your article is not currently listed in the registry it will not appear in the table on this page. We can only deposit data if funders are already listed in the Crossref Funder Registry, but we will pass all funding information on to Crossref so that additional funders can be included in future.

Please check your funding information

The table below contains the information we will share with Crossref so that your article can be found *via* the Funding Data search tool. **Please check that the funder names and grant numbers in the table are correct and indicate if any changes are necessary to the Acknowledgements text.**

Funder name	Funder's main country of origin	Funder ID (for RSC use only)	Award/grant number

Researcher information

Please check that the researcher information in the table below is correct, including the spelling and formatting of all author names, and that the authors' first, middle and last names have been correctly identified. **Names will be indexed and cited as shown on the proof, so these must be correct.**

If any authors have ORCID or ResearcherID details that are not listed below, please provide these with your proof corrections. Please ensure that the ORCID and ResearcherID details listed below have been assigned to the correct author. Authors should have their own unique ORCID iD and should not use another researcher's, as errors will delay publication.

Please also update your account on our online manuscript submission system to add your ORCID details, which will then be automatically included in all future submissions. See here for step-by-step instructions and more information on author identifiers.

First (given) and middle name(s)	Last (family) name(s)	ResearcherID	ORCID iD
Demetra	Giuri		
Marianna	Barbalinardo		
Giovanna	Sotgiu	I-7203-2013	
Roberto	Zamboni		
Morena	Nocchetti		0000-0003-2927-1130
Anna	Donnadio		
Franco	Corticelli		
Francesco	Valle		
Chiara G. M.	Gennari		

Francesca	Selmin		
Tamara	Posati		
Annalisa	Aluigi		0000-0001-8754-7161

Queries for the attention of the authors

Journal: **Nanoscale** Paper: **c8nr10114k**

Title: **Nano-hybrid electrospun non-woven materials made of wool keratin and hydrotalcites as potential bio-active wound dressings**

For your information: You can cite this article before you receive notification of the page numbers by using the following format: (authors), Nanoscale, (year), DOI: 10.1039/c8nr10114k.

Editor's queries are marked like this Q1, Q2, and for your convenience line numbers are indicated like this 5, 10, 15, ...

Please ensure that all queries are answered when returning your proof corrections so that publication of your article is not delayed.

Query Reference	Query	Remarks
Q1	Throughout the manuscript "non-wovens" has been changed to "non-woven materials". Please confirm that the changes are correct.	
Q2	Please confirm that the spelling and format of all author names is correct. Names will be indexed and cited as shown on the proof, so these must be correct. No late corrections can be made.	
Q3	Do you wish to add an e-mail address for the corresponding author? If so, please provide the relevant information.	
Q4	The first line of the Abstract has been inserted as the Graphical Abstract text. Please check that this is suitable. If the text does not fit within the two horizontal lines, please trim the text and/or the title.	
Q5	Please check that the caption of Fig. 2 has been displayed correctly.	
Q6	The sentence beginning "In the hybrid nanofiber..." has been altered for clarity. Please check that the meaning is correct.	
Q7	The sentence beginning "To address the aforementioned..." has been altered for clarity. Please check that the meaning is correct.	
Q8	The sentence beginning "The release profile of..." has been altered for clarity. Please check that the meaning is correct.	
Q9	Citations to Fig. 6 and 7 have been added, please check that the placement of these citations is suitable. If the locations are not suitable, please indicate where in the text the citations should be inserted.	
Q10	The meaning of the word "dispositive" in the sentence beginning "All these..." is not clear - please provide alternative text.	
Q11	The sentence beginning "In particular, the keratin..." has been altered for clarity. Please check that the meaning is correct.	

Q12	The sentence beginning “Moreover, keratin nanofibers…” has been altered for clarity. Please check that the meaning is correct.	
Q13	“Ki” is not cited as an author of ref. 22. Please indicate any changes that are required here.	
Q14	The sentence beginning “The porosity of the nanofiber…” has been altered for clarity. Please check that the meaning is correct.	
Q15	The sentence beginning “At designated time…” has been altered for clarity. Please check that the meaning is correct.	
Q16	The sentence beginning “After incubation times…” has been altered for clarity. Please check that the meaning is correct.	
Q17	Ref. 4: Please check that the initials for the 1st author are displayed correctly.	
Q18	Ref. 7: Please provide the last name for the 1st author.	
Q19	Ref. 32: Please provide the initial(s) for all authors.	

Nanoscale

PAPER

Nano-hybrid electrospun non-woven materials made of wool keratin and hydrotalcites as potential bio-active wound dressings†

Cite this: DOI: 10.1039/c8nr10114k

Demetra Giuri,[a] Marianna Barbalinardo,[b] Giovanna Sotgiu,[a] Roberto Zamboni,[a] Morena Nocchetti,[c] Anna Donnadio,[c] Franco Corticelli,[d] Francesco Valle,[b] Chiara G. M. Gennari,[e] Francesca Selmin,[e] Tamara Posati*[a] and Annalisa Aluigi*[a]

Received 14th December 2018,
Accepted 1st March 2019

DOI: 10.1039/c8nr10114k

rsc.li/nanoscale

In this work, nano-hybrid electrospun non-woven materials made of wool keratin combined with diclofenac loaded hydrotalcites (HTD) were prepared and characterized as potential drug delivery systems and scaffolds for fibroblast cell growth. Nano-hybrid electrospun non-woven materials showed a good adaptability to wet skin, effortlessly conforming to the three-dimensional topography of the tissue. Nanosized HTD exercised an overall reinforcing action on the electrospun non-woven materials since the nanohybrid samples displayed a reduced swelling ratio and a slower degradation profile compared to keratin-based nanofiber non-woven materials containing free diclofenac, without negative effects on drug release. The cell viability test indicated a decreased toxicity of the drug when loaded into nanofibers and confirmed the biocompatibility of keratin/HTD electrospun non-woven materials; moreover, a controlled diclofenac release within the first 24 hours does not compromise the fibroblast cell growth in a significant manner.

Introduction

Bioactive wound dressings are the latest type of biopolymer based membrane, designed to play an important role in promoting the wound healing process. Wound dressings made of nanofiber non-woven materials are considered effective scaffolds for skin tissue regeneration, since their high surface to volume ratio and their microporous structure, which mimics the extracellular matrix (ECM), promote cell adhesion and proliferation.[1,2] Electrospinning is a versatile and straightforward nanotechnology to produce nanofiber non-woven materials by using a high voltage electrostatic field.[3] The electrospun non-woven materials have been widely studied as wound dressings since, besides favouring the cell proliferation, they can be suitably designed to avoid bacterial invasion, to prevent wound surface dehydration and to adsorb wound exudates. In addition, their highly porous structure allows high skin breathability and water vapour permeation.[4] Electrospun non-woven materials can also be efficient drug delivery systems,[5] since (a) the fabrication process allows high drug loading and inhibits the drug recrystallization; (b) the drug release behaviour can be easily modulated by the composition and morphology of nanofibers and (c) the bioavailability of a drug moiety can be easily controlled through designing various dosage forms.[6] In general, biopolymers are preferred for fabrication of bioactive wound dressings due to their enhanced biocompatibility and biodegradation.[7] Until now, the most proposed biopolymers for wound healing were collagen,[8] silk and sericine,[9] cellulose,[10] hyaluronic acid,[11] alginate,[12] chitosan and chitin.[13]

However, in recent years, keratin proteins have also received great attention in the biomedical field. Keratins are naturally abundant non-food proteins found in hair, wool, horns, nails, hooves, reptile scales, bird beaks and feathers. In particular, wool keratin, due to its biodegradability, biocompatibility and bioactivity (linked to the presence of cell adhesion sequences in its primary structure), has been widely explored for the fabrication of scaffolds for tissue engineering and wound healing.[14,15] The electrospinning of wool keratin is generally carried out using organic solvents, such as formic acid[15] or exafluoro-isopropanol.[16] Nevertheless, in the manufacturing process of scaffolds for biomedical applications, the use of organic solvents should be avoided in order to minimize the cytotoxicity risk of the final material. The fabrication of keratin-nanofibers starting from aqueous solution is challen-

[a]Institute of Organic Synthesis and Photoreactivity, National Research Council, via P. Gobetti 101, 40129 Bologna, Italy
[b]Institute of Nanostructured Materials, National Research Council, via P. Gobetti 101, 40129 Bologna, Italy
[c]Dipartimento di Scienze Farmaceutiche, Università degli Studi di Perugia, via del Liceo, 1, 06123 Perugia, Italy
[d]Institute for Microelectronics and Microsystems, National Research Council, via P. Gobetti 101, 40129 Bologna, Italy
[e]Department of Pharmaceutical Sciences, Università degli Studi di Milano, via G. Colombo, 71–20133 Milano, Italy

† Electronic supplementary information (ESI) available: Experimental procedures and a demonstration video. See DOI: 10.1039/c8nr10114k

ging due to their low viscoelastic properties resulting from low molecular weights of the protein. In order to overcome the aforementioned problems, supporting polymers such as polyethylene-oxide (PEO) or polyvinyl alcohol (PVA) are used.[17,18]

The present work aims at designing keratin-based electrospun non-woven materials, loaded with a drug, in order to obtain a bio-active wound dressing that can act, simultaneously, as a scaffold for cell growth and drug delivery systems. Aqueous keratin solutions doped with diclofenac have been electrospun into nanofibers. Diclofenac is a non-steroidal anti-inflammatory drug (NSAID) that inhibits cyclooxygenases, leading to less formation of prostaglandins that cause inflammation and pain. The topical administration of diclofenac has been demonstrated to be capable of reducing phlogistic signals without causing fibroblast or keratinocyte downregulation and thus without leading to excisional wound healing impairment.[19]

PEO was used as a supporting polymer for electrospinning. However, despite the aforementioned advantages of keratin-rich scaffolds, their weak mechanical strength and their fast biodegradation are recognized as the main critical problems that could limit their applications as scaffolds for skin tissue regeneration and controlled drug release. One of the proposed strategies to overcome these problems, successfully used for fibroin and keratin based films,[20,21] is the use of inorganic fillers, such as hydrotalcites. Hydrotalcites (HT) are layered solids with a positively charged surface, balanced by interlayer anions. They are represented by the general formula $[M(II)_{1-x}M(III)_x(OH)_2]^x[A_{x/n}{}^{n-}]mH_2O$ where M(II) is a divalent cation such as Mg, Ni, Zn, Cu, or Co, M(III) is a trivalent cation such as Al, Cr, Fe, or Ga, and A^{n-} is an anion of charge n.[22] The great scientific and technological relevance of HT resides on their tuneable layered charge density, variable chemical composition and rich intercalation chemistry.[23] These advantages, together with their well-known low toxicity and good biocompatibility,[23,24] make HT a very attractive class of layered solids, which find applications in different fields such as medical science,[25,26] polymeric nanocomposites,[20] sensing, and photonic and opto-electronic devices.[27,28] In the last few decades, HT have been increasingly explored as drug carriers. Many anti-inflammatory drugs (*e.g.* ibuprofen and ketoprofen) in the form of anions have been successfully intercalated between the layers of the HT system.[29] The advantages of using HT in the drug delivery field are that they (a) provide drug protection, (b) improve the solubility of the poorly water soluble drug and (c) can modify the drug release profile.[20,22]

In this work, the diclofenac drug was intercalated into the HT (HTD), which in turn dispersed in the keratin solutions and was electrospun into hybrid nanofiber non-woven materials. The effects of HT on the morphology, stability under physiological conditions, and biodegradability in the proteolytic environment of the hybrid keratin-based nanofibers were studied. Afterwards, a systematic study exploring the diclofenac release profiles from keratin/HTD hybrid electrospun non-woven materials and from keratin electrospun non-woven materials doped with free diclofenac was carried out. Finally, the fibroblast cells were grown on the different nanofiber samples with the aim to study the effect of diclofenac release on the cell proliferation and to confirm the biocompatibility of the keratin/HTD system.

Results and discussion

Electrospinning of keratin–HTD solutions

Cysteine-*S*-sulphonated keratin (obtained from wool as described in ESI section I†) and nanosized HT intercalated with anionic diclofenac (D) having the formula $[Zn_{0.68}Al_{0.32}(OH)_2](D)_{0.16}(CO_3)_{0.08}0.67H_2O$ (D content 350 μg mg^{-1}) were used for the preparation of hybrid nanofibers (see ESI section II†).

Based on the results of a previous study, an HTD loading of 10 wt% with respect to keratin (corresponding to 3.5 wt% of diclofenac *vs.* keratin) was considered, since it was found to be the maximum amount achievable in order to obtain a good dispersion of nanosized HT in concentrated keratin solutions.[21]

The keratin aqueous solution (10% w/v) with dispersed HTD could not be electrospun without the addition of a small amount of PEO (2.5% w/v), since the jet broke up into droplets as a result of the low viscosity of the starting solution.[17] Moreover, 0.4 μL of glutaraldehyde per mg of keratin (25 wt%) was added to the solutions before electrospinning in order to improve the stability of keratin/HTD hybrid nanofibers under physiological conditions.

In Fig. 1, the effects of PEO and HTD on the steady shear viscosity of keratin solutions are shown. The Ker(10%)–HTD (1%) solution showed a slight shear thinning at low shear stress and a slight shear thickening at high shear stress. In the considered shear rate range, the mean viscosity was of 6 ± 2 (mPa s). The shear thickening is due to the hydroclustering mechanism, which is an HTD aggregation induced at a critical shear rate.[21] Instead, the initial shear thinning, also reported in the literature for aqueous solutions of bovine serine albumin, was attributed to the rapid formation of a protein

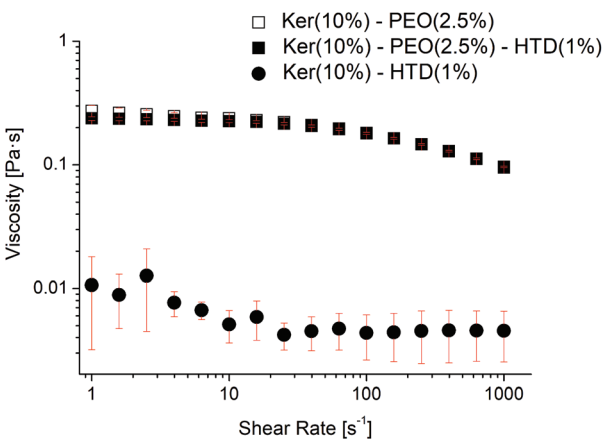

Fig. 1 Logarithmic plot of shear viscosity *versus* shear rate of keratin (10% w/v)–PEO (2.5 w/v), keratin (10% w/v)–HTD (1% w/v) and keratin (10% w/v)–PEO (2.5 w/v)–HTD (1% w/v) solutions, all containing glutaraldehyde 25% (0.4 μg per mg of keratin).

film at the solution/gas interface.[30] This interfacial microstructure of the protein film is disrupted by the larger shear deformation imposed during the steady shear measurements. The addition of PEO increased the viscosity of the solution, thereby allowing its electrospinning. Indeed, when PEO was added to the keratin solution, a typical steady-shear viscosity profile characterized by an initial Newtonian plateau, followed by a shear thinning, appeared. The viscosity evaluated at 16 s^{-1} (within the Newtonian range) reached 23.1 ± 0.9 (mPa s). The steady shear viscosity profile did not change significantly in the presence of HTD. The only notable difference is that the slight shear thinning at a lower shear rate, observable for the Ker(10% w/v)–PEO(2.5% w/v) solution, disappeared in the solution containing hydrotalcites; probably, hydrotalcites interfered with the keratin chain movements, reducing the kinetics of the superficial film formation.

Morphology of the keratin/HTlcD hybrid nanofibers

Keratin/PEO electrospun non-woven materials (KNf-D) loaded with diclofenac (3.5 wt% with respect to keratin) and hybrid keratin/PEO electrospun non-woven materials (KNf-HTD) filled with HTD (10 wt% *vs.* keratin) were prepared. By electrospinning 4 mL of each solution on a 12 × 12 cm^2 metal collector (Fig. 2A), self-standing non-woven materials having a thickness of about 50 μm were obtained (Fig. 2B). Such designed keratin-based electrospun non-woven materials are conceived for applications such as wound dressing and drug delivery systems, since they can be applied to wet skin (Fig. 2C), effortlessly conforming to the three-dimensional topography of the skin (ESI-video†) remaining adherent for at least 24 hours (Fig. 2C and D).

The nanometric structure of the electrospun non-woven materials and the HTD distribution in the nanofibers were analysed by scanning electron imaging using both the secondary electrons (SE) and backscattered electrons (BSE). All the prepared nanofiber non-woven materials were made of randomly oriented and homogeneous nanofibers having a mean diameter of about 295 nm (Fig. 3D and E). In the hybrid nanofiber non-woven material (KNf-HTD), the presence of hydrotalcites embedded into nanofibers was well evident (red circles in the enlarged image of Fig. 3B). Moreover, the bright spots observed in the BSE image, due to the Zn and Al of hydrotalcites (Fig. 3C), demonstrated that the HTD are homogenously distributed and well dispersed inside the nanofibers. Furthermore, XRD patterns, given in Fig. 3F, indicate that the dispersed HTD retain their typical lamellar structure after electrospinning in the presence of diclofenac anions in the interlayer region. Importantly, the hydrotalcites did not significantly change the physical characteristics of the nanofiber non-woven materials in terms of mean fiber diameter, diameter distribution, thickness, porosity and specific surface area (Table 1). The porosity of a scaffold for tissue engineering is a critical parameter since it determines its ability for cell adhesion, migration and also for the exchange of nutrients between the 3D construct and the surrounding environment. As shown in Table 1, the porosity of the keratin-based electrospun membranes fell within 60–90%, which is the preferred range for a scaffold to ensure fibroblast cell penetration.[31]

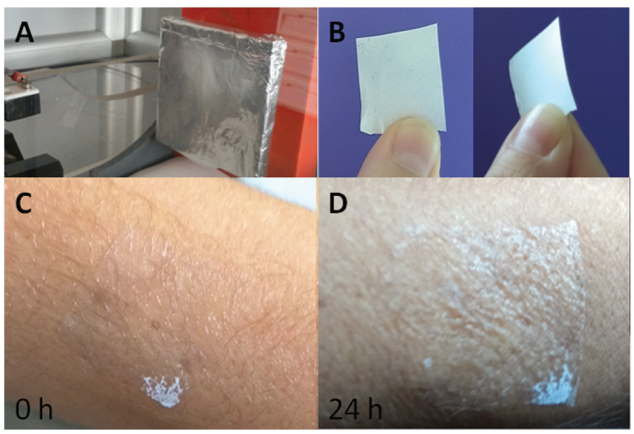

Fig. 2 Electrospinning process (A), keratin–PEO–HTD hybrid nanofiber non-woven materials (B), deposited on wet skin at time 0 h (C) and after 24 hours (D).

Swelling ratio and water stability

The swelling ratio of the electrospun non-woven materials is fundamental to understand the capacity of these materials to adsorb wound exudates usually produced during the inflammatory phase of the healing process. To accomplish that, the KNf-D and KNf-HTD samples were incubated in a PBS solution at 37 °C and their morphology and weight were monitored after 24 hours of incubation. The test was also carried out on the KNf-HT sample, in order to evaluate the effect of diclofenac on the swelling behaviour. Both electrospun non-woven materials tended to swell in PBS at 37 °C, without dissolving themselves. In Fig. 4A–C, the morphology of the KNf-HTD hybrid non-woven materials before and after the immersion is represented as an example. As is shown, the samples retained their fibrous and porous structure (Fig. 4B and C) although they have lost their original morphology due to the nanofiber swelling. The swelling ratio of the KNf-D membrane (~20 ± 2) was higher than that of the KNf-HTD membrane (~12 ± 1). In contrast, the swelling ratio of the KNf-HT sample (11 ± 1) was not significantly different from that of KNf-HTD, thereby demonstrating that the behavior of the hybrid sample was unaffected by the presence of diclofenac. This reinforcing action of HTD, also observed in keratin-based[21] and fibroin-based films[20] probably results from the chemical interactions between the protein functional groups (C═O and N–H) and hydroxyl groups of hydrotalcites, which reduce the mobility of the protein chains.

Biodegradability

Most of the commercially available wound dressings are non-biodegradable and therefore they need to be removed from the wound. Such removal can affect the wound healing process, inducing the formation of scar tissue and increasing the risk of bacterial contamination.[31] To address the aforementioned issue, research efforts have been made towards the design of biodegradable wound dressings. However, to be functional for

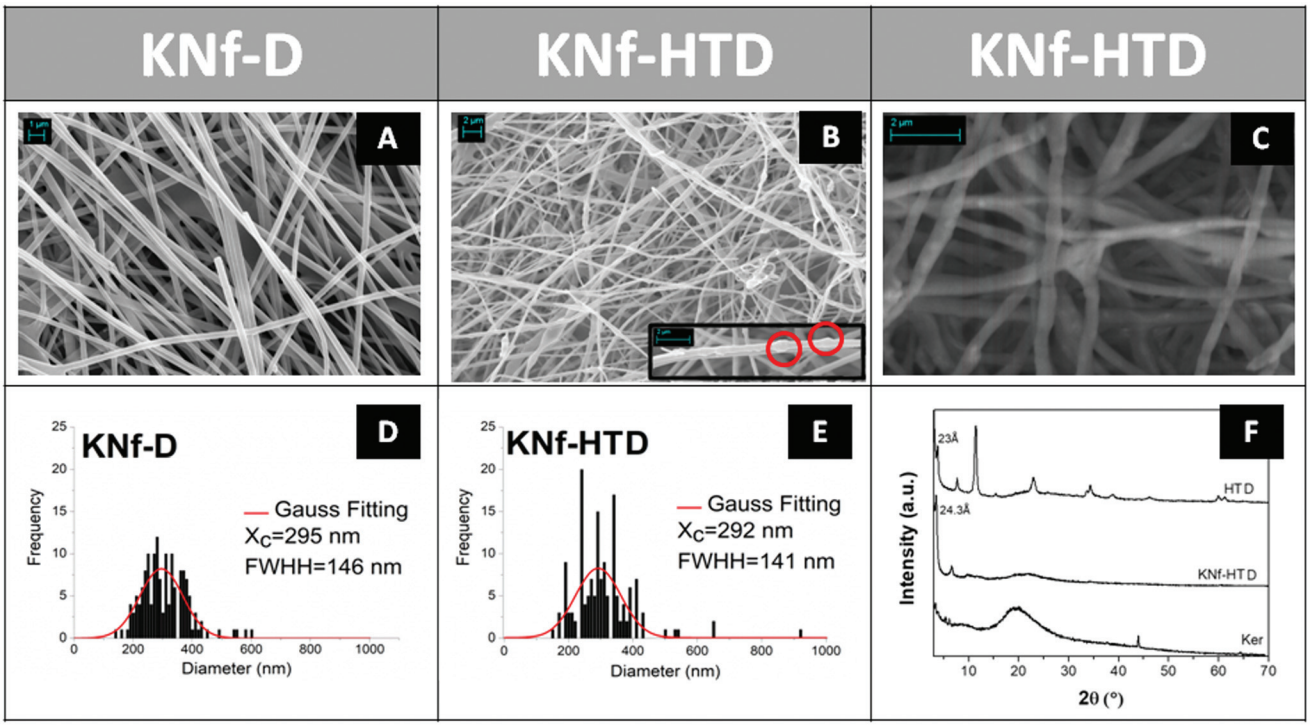

Fig. 3 SEM images observed with secondary electrons (SE) of (A) keratin-based nanofiber non-woven materials loaded with free diclofenac (KNf-D), (B) keratin-based hybrid nanofiber non-woven materials filled with diclofenac loaded hydrotalcites (KNf-HTD) (C) backscattered electrons (BSE) of KNf-HTD, diameter distributions of (D) KNf-D and (E) KNf-HTD; and (F) X-ray diffraction pattern of HTD, KNf-HTD and keratin.

Table 1 Chemical–physical parameters of nanofiber non-woven materials

Parameters/material	KNf-D	KNf-HTD
[HTD] (%)	#	10
[Diclofenac] (%)	3.5	3.5
Thickness (μm)	57 ± 2	54 ± 2
Porosity (%)	79 ± 1	80 ± 1
Specific surface area ($m^2\ g^{-1}$)	10	11

tissue regeneration, a wound dressing should have a degradation rate comparable to the regeneration rate of the compromised tissue.[32] In Fig. 5, the biodegradability profiles of KNf-D and KNf-HTD samples, incubated at 37 °C in a solution of protease XIV in PBS saline buffer (pH 7.4), are compared. As can be observed, the KNf-D membranes showed a rapid weight loss of 50% in the first 24 hours of exposure to protease. The degradation is almost complete (97%) after 48 hours. Differently, the hybrid nanofibers showed a higher resistance

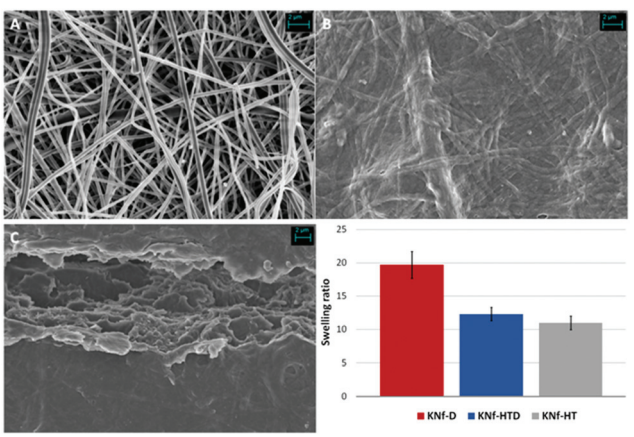

Fig. 4 SEM images of (A) KNf-HTD, (B) KNf-HTD after the immersion in the PBS solution at 37 °C for 24 hours and (C) related section, and (D) comparison between the swelling ratio of KNf-D and KNf-HTD.

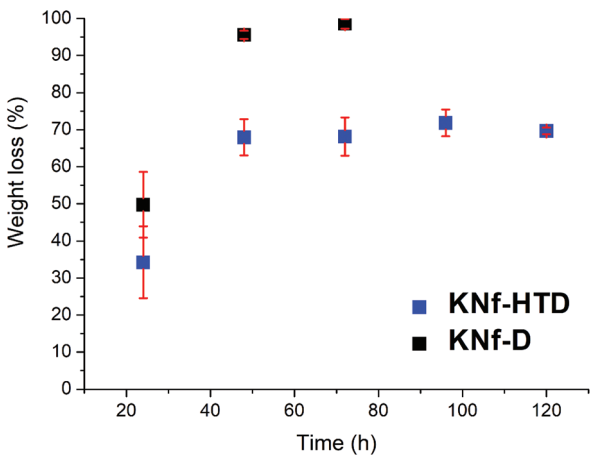

Fig. 5 Comparison of *in vitro* biodegradation profiles of KNf-D and KNf-HTD electrospun non-woven materials.

to enzymatic degradation; indeed, their weight loss was about 30% after 24 hours, and it reached 67% after 48 h and remained constant for 120 hours. This reinforcing action of hydrotalcites, conferring an enhanced protease resistance to the hybrid electrospun non-woven materials, makes them more suitable to address the inflammatory and proliferative phases of the skin regeneration process.

Drug release kinetic study

The profiles of the cumulative percentages of diclofenac permeating through Cuprophan® were almost superimposable throughout the experiment with the exception of some early data points (at 45 min and 1 h, $p < 0.05$). Overall, these patterns indicate that the presence of hydrotalcites did not influence the drug release from the samples. The release profile of diclofenac from both formulations fits Higuchi's model ($R^2 >$ 0.99) and the drug release was controlled by diffusion with similar rates, as shown in Table 2. To find out the mechanism of drug release, the data were fitted in the Korsmeyer–Peppas equation. In this model, the value of "n", *i.e.* the release exponent, described the mode of the transport mechanism.[33] In both cases, the fitting indicates the combined effect of diffusion and relaxation mechanisms for the release which deviates from the Fick equation, following a non-Fickian (anomalous) transport.[33] The experimental release data were also fitted to the Peppas–Sahlin model[33] which describes the drug release kinetics from hydrophilic polymers and is applicable for different geometric shapes (Table 2). The model considers the release kinetics to be affected by two additive transport mechanisms: Fickian diffusional release (k_d) and case-II relaxational contribution (k_d) as illustrated in eqn (7). The values of the coefficient of determination R^2 were equal to or above 0.95 for all the films. In the case of KNf-D, the ratio between k_d and k_r was close to 1, suggesting that both transport mechanisms controlled the diclofenac release. Regarding $K_{Nf\text{-}HTD}$, the values of k_r were very small (k_r = 0.028 ± 0.05 $h^{-0.45}$), indicating that the case II relaxation has no significant contribution in the release process. At the same time, the values of the Fickian diffusion contribution constants (k_d = 0.253 ± 0.071 $h^{-0.45}$) were higher than k_r. Moreover, they were even higher than k_d of KNf-D samples, suggesting a faster drug diffusion through the electrospun matrix in the presence of HT. This comparison among the two K_d can justify the small differences observed between the two formulations in the release pattern at the early data points (Fig. 6).

Table 2 Parameters and correlation coefficient for Higuchi, Korsmeyer–Peppas and Peppas–Sahlin models

Model/sample	KNf-HTD	KNf-D
Higuchi		
K (μg cm^{-2} $h^{1/2}$)	0.33 ± 0.08	0.33 ± 0.03
R^2	>0.99	>0.99
Korsmeyer–Peppas		
N	0.53 ± 0.04	0.81 ± 0.04
R^2	>0.90	>0.93
Peppas–Sahlin		
k_d ($h^{-0.45}$)	0.25 ± 0.07	0.10 ± 0.02
k_r ($h^{-0.45}$)	0.028 ± 0.05	0.11 ± 0.03
R^2	>0.95	>0.95

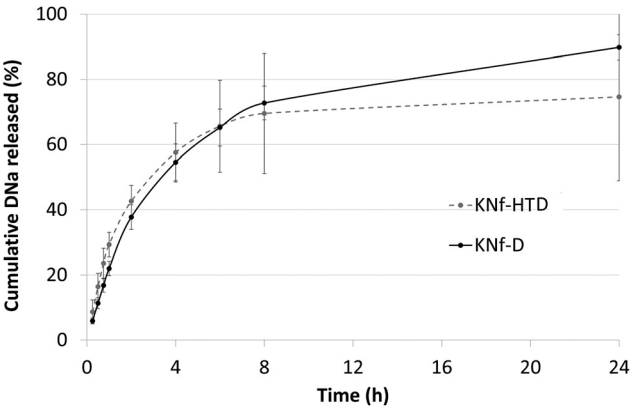

Fig. 6 Cumulative diclofenac released from KNf-HTD (dotted line) and KNf-D (black line).

Evaluation of cell viability and proliferation

The wound healing process is known by its complexity and interaction of different cell types with matrix components that act together to re-establish the 3D structure and the functions of the damaged tissue. Herein, NIH-3T3 cells were used to evaluate the cell response to the presence of the developed membranes. In order to evaluate both the effect of drug release on cell viability and the effect of nanofibers on drug performances, the tests were carried out on free diclofenac (D), hybrid electrospun non-woven materials (KNf-HTD), hybrid nanofibers containing HT without diclofenac (KNf-HT) and diclofenac loaded keratin nanofibers without HT (KNf-D). As

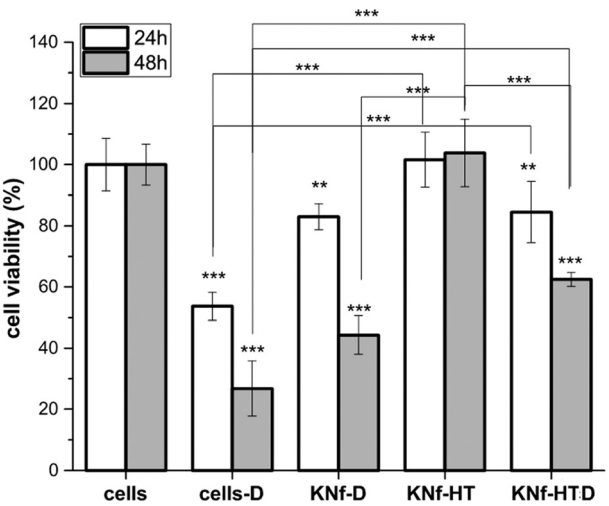

Fig. 7 Cell viability of NIH-3T3 on diclofenac (cell-D), KNf-D, KNf-HT, and KNf-HTD. Data represent the mean ± standard deviation. Statistical analyses were performed using ANOVA followed by Tukey's test. ***$p \leq$ 0.001 and **$p \leq$ 0.005 denote significant differences with respect to the control.

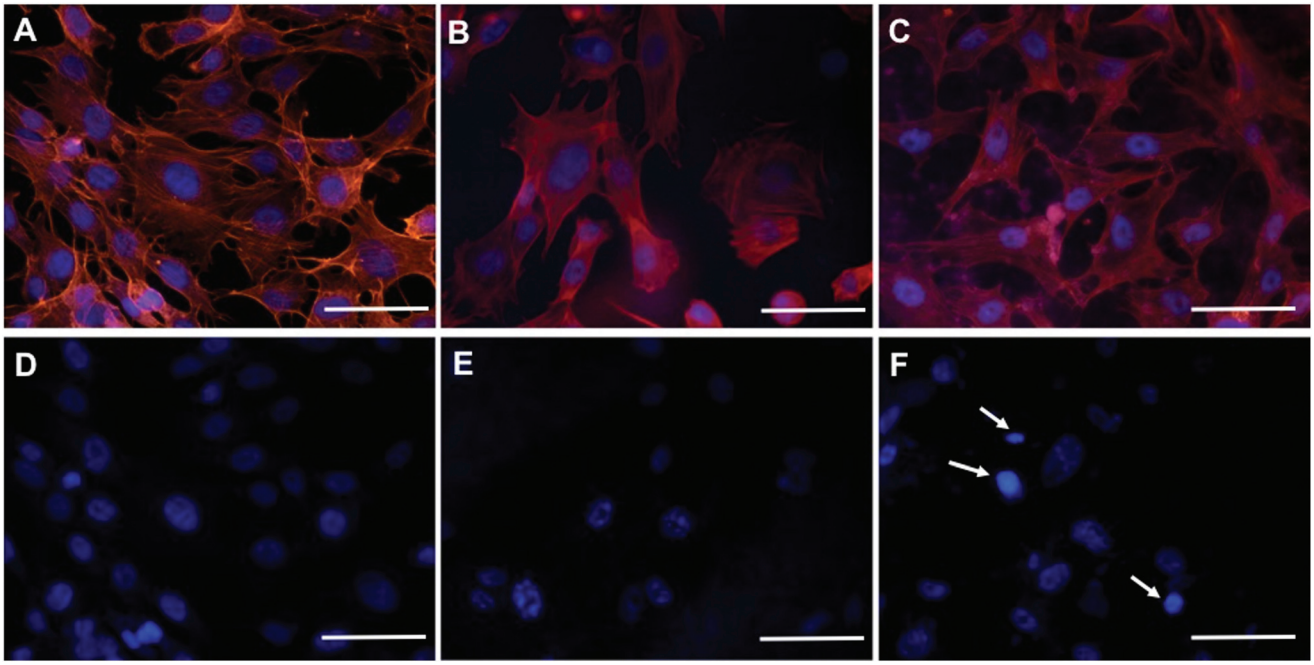

Fig. 8 Fluorescence micrographs of NIH-3T3 (A) on glass, (B) on KNf-HT and (C) on KNf-HTD; cells labeled specifically for actin (red) and the nucleus (blue) after 48 h of incubation. Chromatin condensation of NIH-3T3 cells stained with DAPI after 48 h (D) on glass, (E) on KNf-HT, and (F) on KNf-HTD. Fluorescence micrographs showed fragmented and condensed nuclei as indicated by an arrow.

expected, the free drug displayed a significant toxic effect on fibroblasts,[34] reducing the cell viability to about 54 ± 5% within the first 24 hours and 27 ± 9% after 48 hours. Differently, the toxicity was reduced (cell growth 83 ± 4% after 24 hours and 44 ± 6% after 48 hours), when the drug release is mediated by nanofibers (KNf-D) (Fig. 7).

Regarding hybrid samples, HT did not display toxic effects towards NIH-3T3 cells (KNf-HT). Indeed, fibroblast growth scattered and formed discrete groups in KNf-HT hybrid electrospun non-woven materials. On the other hand, a decrease in fibroblast growth at 48 h was observed on KNf-HTD nanofiber nonwovens (Fig. 8A–C). Specifically, at 24 hours the cell growth was comparable to that of the control (85 ± 10%), proving that the mitochondrial activity is not compromised by diclofenac. Instead, at 48 hours, a significant cell growth reduction occurred (63 ± 2%), confirming the well-known inhibitory effect of the drug. However, this negative effect was significantly pronounced when the drug is not intercalated in the hydrotalcites (KNf-D). Notably, the higher antiproliferative effect of diclofenac after 48 hours occurs because the tests have been performed without replacing the medium, causing drug accumulation during the experiment time.[34,35]

Conclusions

Electrospun non-woven materials based on keratin nanofibers (~292 nm) loaded with diclofenac and hybrid nanofibers (295 nm) made of keratin and hydrotalcites intercalated with diclofenac were successfully prepared by electrospinning.

Based on the obtained results, the presence of hydrotalcites reduced the swelling ratio and decreased the biodegradation kinetics of the electrospun non-woven materials. Both electrospun non-woven materials displayed a sustained diclofenac release over 24 hours and the hybrid samples showed a lower contribution of matrix relaxation in the release mechanism. The cell viability tests revealed that the keratin/hydrotalcites electrospun non-woven materials are not toxic and support the fibroblast cell growth. It has been demonstrated that when the diclofenac is released in a controlled manner within the first 24 hours, it does not display its well-known antiproliferative effect. All these preliminary results obtained in this work are fundamental for a biomedical dispositive design with drug loading, drug release times and biodegradation kinetics suitable for personalized wound care treatment.

Experimental

Materials

Australian Merino wool (21 μm fineness) was kindly supplied by Cariaggi Fine Yarns, S.p.A. All other chemicals were purchased from Sigma-Aldrich and used without further purification.

Preparation of KNf-D, KNf-HT and KNf-HTD electrospun non-woven materials

Keratin was extracted from Merino wool (21 μm) by sulphitolysis reaction and the HTD nanoparticles were first obtained in the bromide form by the double-microemulsion technique[21]

and successively intercalated with anionic diclofenac (350 μg mg^{-1}) by ionic exchange reaction.[22] The procedures related to the keratin extraction and HTD synthesis are reported in the ESI (sections I and II†).

For the preparation of diclofenac loaded nanofibers, conventional home-made electrospinning apparatus composed of an high voltage generator (ALINTEL SHV 150, 5 mA, ±30 kV), a precision syringe pump (KdScientific), a plastic syringe with a stainless-steel needle (18 Gauge) and an aluminium and static collector was used. In particular, the keratin/HTD hybrid nanofiber non-woven materials (KNf-HTD) were prepared by electrospinning the keratin solution (10% w/v), containing poly(ethylene-oxide) (PEO, 2,5% w/v), glutaraldehyde 25% (0.4 μL per mg of keratin) and 1% w/v of HTD (10 wt% *vs*. keratin, corresponding to 35 mg of diclofenac per gram of nanofiber non-woven material). Moreover, keratin nanofibers loaded with free diclofenac (KNf-D) were prepared by electrospinning the keratin solution (10 wt%) containing 0.35% w/v of diclofenac (corresponding to 35 mg per gram of nanofiber non-woven material). For the cell viability tests, a keratin solution (10% w/v) containing poly(ethylene-oxide) (PEO, 2,5% w/v), glutaraldehyde 25% (0.4 μL per mg of keratin) and 1% w/v of HT without diclofenac was also electrospun. All the prepared solutions were electrospun using a voltage of 20 kV, a flow rate of 0.05 mL min^{-1} and a needle-collector distance of 15 cm.

Nanofiber non-woven materials characterization

The solutions were characterized from the rheological point of view, carrying out shear rate-dependent viscosity measurements, using an Anton Paar Compact Rheometer MCR 102 equipped with a PDT 200/56/l Peltier temperature control device, set at 25 (±0.1)°C, using a cone plate geometry (75 mm diameter, 1° angle and 45 μm truncation), in controlled shear rate mode. The shear rate was logarithmically increased from 1 to 1000 s^{-1}. Data were acquired and elaborated with the RheoCompass™ Software (Anton Paar GmbH). The electrospun nanofiber morphology was observed under a scanning electron microscope (SEM) using a Zeiss EVO LS 10 LaB6 scanning electron microscope, with an acceleration voltage of 5 kV and a working distance of 5 mm. Samples were gold-sputtered for 1 min before the analysis. The fiber diameters were analyzed by means of freely distributed software GIMP 2.8 (GNU Image Manipulation Program). In particular, the mean diameter and the diameter distribution of nanofibers were evaluated from 100 measurements randomly gathered from several SEM photos of several nanofiber non-woven materials. The thickness of keratin nanofibrous membranes was measured by using a digital micrometer (Mitutoyo, IP65).

XRD patterns were obtained with a Philips X'PERT PRO MPD diffractometer operating at 40 kV and 40 mA with a step size 0.0170 $2\theta°$ and a step scan of 20 s, using Cu Kα radiation and an X'Celerator detector.

The porosity and the specific surface area of the keratin nanofiber membranes were calculated on a square sample of 4 cm^2 as suggested by Ki *et al.*[22] Practically, assuming nanofilaments as cylinders of indefinite length, the specific surface area S can be calculated using the following eqn (1):

$$S = \frac{4}{\rho D} \quad (1)$$

where D (cm) is the mean diameter of the nanofibers and ρ (g cm^{-3}) is the density of the nanofiber non-woven materials. The density and the porosity of the nanofiber non-woven materials were determined through a liquid displacement method.[36]

Practically, the density of the nanofiber mat was calculated by using the mass of the mat in air (m_1) and in *n*-hexane (m_2) through the following eqn (2):

$$\rho = \frac{m_1 \rho_h}{(m_1 - m_2)} \quad (2)$$

where ρ_h is the density of *n*-hexane at a temperature of the measurement. The porosity of the nanofiber non-woven materials is obtained by using eqn (3):

$$\varepsilon = \frac{(V_{TOT} - V)}{V_{TOT}} \quad (3)$$

where V_{TOT} is the total (apparent) volume, obtained by measuring the area and the thickness of the nanofiber non-woven material and V is the volume, calculated from the measured mass and density of the nanofiber non-woven material. For swelling studies, samples were dried at 40 °C for 3 h and weighed (w_D g^{-1}). Afterwards, they were immersed in PBS at pH 7.4 (liquor ratio of 4 mg mL^{-1}), at 37 °C for 2 h. The supernatant was removed and the wet samples were weighed (w_w g^{-1}). The swelling ratio (SD) was calculated using the following eqn (4):

$$\text{Swelling ratio} = \frac{(W_w - W_D)}{w_w} \quad (4)$$

For the evaluation of the sample biodegradation, the nanofiber non-woven materials were incubated at 37 °C in protease XIV (protease from *Streptomyces griseus* type XIV, ≥3.5 units mg^{-1} solid Sigma) in phosphate buffer saline (PBS), at pH 7.4. 2.5 μg of protease per mg of keratin was considered. At designated time points, groups of samples were centrifuged, rinsed first with distilled water and then with acetone and dehydrated at 50° overnight. After oven removal, the samples were weighed to estimate the extent of degradation.

Drug release test

In vitro release studies were performed using Franz diffusion cells (permeation area: 0.636 cm^2; volume of receptor chamber about 3 mL) and Cuprophan® as the synthetic release membrane. Prior to experiments, the Cuprophan® membrane was hydrated in 0.9% w/v NaCl solution for 1 h. At the beginning of the experiment, formulations (2.54 cm^2) were applied to the surface of the Cuprophan® membrane. Then, the sample was mounted on the Franz diffusion cells, whose receptor compartments were filled with degassed 0.9% w/v NaCl solution. Special care was given to avoid air bubbles between the membrane and the solution in the receptor compartment. The

upper and lower parts of the Franz cell were sealed with Parafilm® and fastened together by means of a clamp. The system was kept at 37 °C with a circulating water bath, so that the membrane surface temperature was at 32 ± 1 °C throughout the experiment. At predetermined times (15, 30, 45 min, 1, 2, 4, 6, 8 and 24 h), 200 μL samples were withdrawn from the receiver compartment and analysed by HPLC. The withdrawn aliquot was replaced with the same volume of the fresh receiver medium. Sink conditions were maintained throughout the experiments. The results were expressed as the average of parallel experiments performed in triplicate. The cumulative amount released ($Q_{R,t}$) from the formulations per unit area was calculated from the drug concentration in the receiving medium and plotted as a function of time. The release data were analyzed according to the Higuchi equation,[37] eqn (5), the Korsmeyer–Peppas equation model,[33] eqn (6), and the Peppas–Sahlin equation,[38] eqn (7). All equations were applied for $M_t/M_f < 0.6$.[39] The nonlinear least squares fitting method was used to determine the parameters in each equation.

$$\frac{M_t}{M_f} = k \times t^{0.5} \quad (5)$$

$$\frac{M_t}{M_f} = k' \times t^{n} \quad (6)$$

$$\frac{M_t}{M_f} = k_d \times t^{m} + k_r \times t^{2m} \quad (7)$$

where M_t is the concentration of diclofenac released at time t, M_f is the concentration of diclofenac released at equilibrium, k and k' are constants incorporating the structural and geometric characteristics of the matrices, n is the release exponent describing the mode of the transport mechanism, and m is the purely Fickian diffusion exponent for a system of any geometrical shape.

The amount of diclofenac sodium was determined by high performance liquid chromatography (HPLC; HP 1100 ChemStations, Agilent Technologies, Santa Clara, US), equipped with an ultraviolet detector at 254 nm (ref. 40). Phosphate buffer (0.01 M) pH 2.5/methanol (34/66, v/v) was used as the mobile phase at a flow rate of 1.2 mL min^{-1} and the analysis temperature was fixed at 45 °C. The compound separation was carried out using a reverse-phase column (InertClone™, 5 μm, 150 × 4.6 mm, Phenomenex, US) and the injection volume was set at 10 μL. The retention time of diclofenac sodium was about 9.8 min and a calibration curve was constructed in the range of 0.2–50 μg mL^{-1}.

Cell cultures

Mouse embryonic fibroblast (NIH-3T3/GFP) cells were cultured under standard conditions in the DMEM medium, supplemented with 10% (v/v) FBS, 2 mM L-glutamine, 0.1 mM MEM Non-Essential Amino Acids (NEAA), 100 U mL^{-1} penicillin and 100 U mL^{-1} streptomycin in a humidified incubator set at 37 °C with 5% CO_2. Cells were seeded on keratin in 24-well plates at a density of 105 cells per cm^2.

Actin and nucleus staining

Cells were fixed with 4% paraformaldehyde in DPBS and washed with DPBS. They were then permeabilized with 0.001% Triton-X 100. The cells were labelled with TRITC-conjugated phalloidin (FAK100, Merck Millipore) for 1 h, followed by rinses with DPBS. Actin staining was critical to map the local orientation of actin filaments within cells. Nuclear counterstaining was performed by incubation with DAPI (FAK100, Merck Millipore) for 3 min, followed by rinses with DPBS. Samples were examined using a Nikon Eclipse 80i microscope equipped for fluorescence analysis.

Cells viability (resazurin reduction assay)

Cell viability was determined by resazurin reduction assay; the reagent is an oxidized form of the redox indicator that is blue in colour and non-fluorescent. When incubated with viable cells, the reagent is reduced and it changes its colour from blue to red becoming fluorescent. Briefly, cells were seeded on free diclofenac D (105 μg, 0.66 mM) and 3 mg of KNf-D, KNf-HT and KNf-HTD with complete medium. The used free diclofenac was calculated on the basis of that loaded in the nanofibers used in the test. After incubation times, the resazurin reagent was added directly to the culture medium with 10% volume of medium contained in each sample and incubated for 3 h at 37 °C with 5% CO_2. Subsequently, aliquots from each sample were transferred to a 96 multiwell plate for fluorescence measurement at λ_{exc} 560 nm and λ_{em} 590 nm (Thermo Scientific Varioskan Flash Multimode Reader). We included a negative control of only medium without cells to determine the background signal and a positive control of 100% reduced resazurin reagent without cells.

Conflicts of interest

The authors declare no conflict of interest.

Acknowledgements

The authors acknowledge Lanificio Cariaggi Fine Yarns for the supply of Merino Wool fibres.

Notes and references

1 M. Abrigo, S. L. McArthur and P. Kingshott, *Macromol. Biosci.*, 2014, **14**, 772–792.
2 T. D. Stocco, N. J. Bassous, S. Zhao, A. E. C. Granato, T. J. Webster and A. O. Lobo, *Nanoscale*, 2018, **10**, 12228–12255.
3 C. J. Thompson, G. G. Chase, A. L. Yarin and D. H. Reneker, *Polymer*, 2007, **48**, 6913–6922.
4 G. V. C. P. R. E. Brewster, *Pharm. Res.*, 2003, **20**, 810–817.
5 Y.-F. Goh, I. Shakir and R. Hussain, *J. Mater. Sci.*, 2013, **48**, 3027–3054.

6 Q. Wang, N. Zhang, X. Hu, J. Yang and Y. Du, *Eur. J. Pharm. Biopharm.*, 2007, **66**, 398–404.

7 D. Y. and J. Fisher, in *Biomedical Materials*, ed. S. Narayan, New York, NY., 2009, pp. 415–442. Q18

8 N. Hild, O. D. Schneider, D. Mohn, N. A. Luechinger, F. M. Koehler, S. Hofmann, J. R. Vetsch, B. W. Thimm, R. Müller and W. J. Stark, *Nanoscale*, 2011, **3**, 401–409.

9 S. Gilotra, D. Chouhan, N. Bhardwaj, S. K. Nandi and B. B. Mandal, *Mater. Sci. Eng., C*, 2018, **90**, 420–432.

10 Y. Liu, J. Vincent Edwards, N. Prevost, Y. Huang and J. Y. Chen, *Mater. Sci. Eng., C*, 2018, **91**, 389–394.

11 Y. Qian, L. Li, C. Jiang, W. Xu, Y. Lv, L. Zhong, K. Cai and L. Yang, *Int. J. Biol. Macromol.*, 2015, **79**, 133–143.

12 H. Hajiali, M. Summa, D. Russo, A. Armirotti, V. Brunetti, R. Bertorelli, A. Athanassiou and E. Mele, *J. Mater. Chem. B*, 2016, **4**, 1686–1695.

13 F. Ding, H. Deng, Y. Du, X. Shi and Q. Wang, *Nanoscale*, 2014, **6**, 9477–9493.

14 P. Hill, H. Brantley and M. Van Dyke, *Biomaterials*, 2010, **31**, 585–593.

15 S. Xu, L. Sang, Y. Zhang, X. Wang and X. Li, *Mater. Sci. Eng., C*, 2013, **33**, 648–655.

16 S. Ferraris, V. Guarino, A. Cochis, A. Varesano, I. Cruz Maya, C. Vineis, L. Rimondini and S. Spriano, *Mater. Lett.*, 2018, **229**, 1–4.

17 A. Aluigi, C. Vineis, A. Varesano, G. Mazzuchetti, F. Ferrero and C. Tonin, *Eur. Polym. J.*, 2008, **44**, 2465–2475.

18 Y. Esparza, A. Ullah, Y. Boluk and J. Wu, *Mater. Des.*, 2017, **133**, 1–9.

19 F. L. da S. Costa, L. D. Tiussi, M. S. Nascimento, A. C. de S. Corrêa, E. Y. Yasojima and C. A. A. Pires, *Acta Cir. Bras.*, 2014, **29**, 328–333.

20 T. Posati, V. Benfenati, A. Sagnella, A. Pistone, M. Nocchetti, A. Donnadio, G. Ruani, R. Zamboni and M. Muccini, *Biomacromolecules*, 2014, **15**, 158–168.

21 T. Posati, D. Giuri, M. Nocchetti, A. Sagnella, M. Gariboldi, C. Ferroni, G. Sotgiu, G. Varchi, R. Zamboni and A. Aluigi, *Eur. Polym. J.*, 2018, **105**, 177–185.

22 L. Perioli, T. Posati, M. Nocchetti, F. Bellezza, U. Costantino and A. Cipiciani, *Appl. Clay Sci.*, 2011, **53**, 374–378.

23 A. I. Khan and D. O'Hare, *J. Mater. Chem.*, 2002, **12**, 3191–3198.

24 T. Posati, A. Pistone, E. Saracino, F. Formaggio, M. G. Mola, E. Troni, A. Sagnella, M. Nocchetti, M. Barbalinardo, F. Valle, S. Bonetti, M. Caprini, G. P. Nicchia, R. Zamboni, M. Muccini and V. Benfenati, *Sci. Rep.*, 2016, **6**, 31226.

25 Z. Wang, P. Liang, X. He, B. Wu, Q. Liu, Z. Xu, H. Wu, Z. Liu, Y. Qian, S. Wang and R. Zhu, *Nanoscale*, 2018, **10**, 13106–13121.

26 Y. Wu, R. Zhu, Y. Zhou, J. Zhang, W. Wang, X. Sun, X. Wu, L. Cheng, J. Zhang and S. Wang, *Nanoscale*, 2015, **7**, 11102–11114.

27 L. Chen, K. Sun, P. Li, X. Fan, J. Sun and S. Ai, *Nanoscale*, 2013, **5**, 10982.

28 T. Posati, M. Melucci, V. Benfenati, M. Durso, M. Nocchetti, S. Cavallini, S. Toffanin, A. Sagnella, A. Pistone, M. Muccini, G. Ruani and R. Zamboni, *RSC Adv.*, 2014, **4**, 11840.

29 V. Ambrogi, G. Fardella, G. Grandolini and L. Perioli, *Int. J. Pharm.*, 2001, **220**, 23–32.

30 V. Sharma, A. Jaishankar, Y.-C. Wang and G. H. McKinley, *Soft Matter*, 2011, **7**, 5150.

31 Y.-C. Jiang, L. Jiang, A. Huang, X.-F. Wang, Q. Li and L.-S. Turng, *Mater. Sci. Eng., C*, 2017, **71**, 901–908.

32 Zhang, Duan, Feng, Guo, Wang, Zhao, Zhou, Wei and Cao, *Int. J. Nanomed.*, 2013, 2077. Q19

33 R. W. Korsmeyer, R. Gurny, E. Doelker, P. Buri and N. A. Peppas, *Int. J. Pharm.*, 1983, **15**, 25–35.

34 M. S. M. Al-Nimer, H. G. Hameed and M. M. Mahmood, *Saudi Pharm. J.*, 2015, **23**, 483–486.

35 F. Albano, A. Arcucci, G. Granato, S. Romano, S. Montagnani, E. De Vendittis and M. R. Ruocco, *Biochimie*, 2013, **95**, 934–945.

36 B. P. Antunes, A. F. Moreira, V. M. Gaspar and I. J. Correia, *Carbohydr. Polym.*, 2015, **130**, 104–112.

37 T. Higuchi, *J. Pharm. Sci.*, 1963, **52**, 1145–1149.

38 N. A. Peppas, *Pharm. Acta Helv.*, 1985, **60**, 110–111.

39 N. A. Peppas and J. J. Sahlin, *Int. J. Pharm.*, 1989, **57**, 169–172.

40 P. Minghetti, F. Cilurzo, A. Casiraghi, L. Montanari and A. Fini, *J. Pharm. Sci.*, 2007, **96**, 814–823.